Frontiers in Heat and Mass Transfer (FHMT), 2, 043005 (2011)
DOI: 10.5098/hmt.v2.4.3005

Global Digital Central
ISSN: 2151-8629

Frontiers in Heat and Mass Transfer

Available at www.ThermalFluidsCentral.org

THERMAL PERFORMANCE ENHANCEMENT OF PARAFFIN WAX WITH AL_2O_3 AND CuO NANOPARTICLES – A NUMERICAL STUDY

A. Valan Arasu[a,*] Agus P. Sasmito[b,†], Arun S. Mujumdar[b]

[a] *Department of Mechanical Engineering, Thiagarajar College of Engineering, Madurai-625015, Tamilnadu, India*
[b] *Department of Mechanical Engineering, National University of Singapore, 10 Kent Ridge Crescent, Singapore 119260, Singapore*

ABSTRACT

The heat transfer enhancement of paraffin wax, a cheap and widely used latent heat thermal energy storage material, using nanoparticles is investigated. The effects of nanoparticle volume fraction on both the melting and solidification rates of paraffin wax are analysed and compared for Al_2O_3 and CuO nanoparticles. Present results show that dispersing nanoparticles in smaller volumetric fractions increase the heat transfer rate. The enhancement in thermal performance of paraffin wax is greater for Al_2O_3 compared with that for CuO nanoparticles. .

Keywords: *thermal storage; phase change material; paraffin wax; melting; solidification; nanoparticle.*

1. INTRODUCTION

Well designed energy storage systems not only reduce the mismatch between supply and demand but also improve the performance and reliability of energy systems and can play an important role in conserving energy. Thermal energy can be stored in the form of sensible heat and/or latent heat. Of the two, the latent heat thermal energy storage (LHTS) technique has proved to be a better engineering option due to its various advantages such as large energy storage for a given volume, uniform energy storage/supply, compactness, etc. LHTS units employ phase change materials (PCMs), which undergo phase change (solid-to-liquid and vice versa) during the energy transfer process. Numerous PCMs with their properties, advantages and limitations have been comprehensively reported in Refs. (Sharma and Sagara, 2005; Zalba et al., 2003; Kenisarin and Mahkamov, 2007).

LHTS units have the potential to serve as promising energy storage devices due to high thermal energy density and isothermal heat transfer process. Nevertheless, the low heat flux achieved due to the low thermal conductivity of most phase change materials, which drastically affects the melting and solidification performance of the system, widespread use of latent heat stores has not yet been realised.

A larger heat flux can be achieved by enhancing the effective thermal conductivity. Different approaches have been proposed to overcome this problem: use of metal thin strips (Hoogendoorn and Bart, 1992), thin walled rings (Velraj *et al*. 1999), porous metals (Weaver and Viskanta, 1986) porous graphite (Tayeb, 1996), metal foam matrix (Calmidi and Mahajan, 1999) and carbon fibers (Fukai *et al.* 2000 and 2002) are among the common techniques used to enhance the effective thermal conductivity of PCMs. The presence of the nanoparticles in the PCM increases significantly the effective thermal conductivity of the fluid and consequently enhances the heat transfer characteristics (Cabeza et al. , 2002; Mettawee, and Assassa, 2007; Khodadadi, and Hosseinizadeh, 2007; Zeng *et al*. 2007; Pincemin *et al*., 2008; Kim and Drzal, 2009; Ho and Gao, 2009).

In the present work, a numerical investigation is carried out to estimate the effect on thermal performance of paraffin wax due to the enhancement in thermal conductivity using alumina(Al_2O_3) and copper oxide (CuO) nanoparticles. The effect of volumetric concentration of the nanoparticles on the melting and solidification performance is examined.

2. MODEL FORMULATION

The physical model consists of a rectangular channel (60 cm x 1 cm) carrying water as the heat transfer fluid (HTF), surrounded by a PCM channel (60 cm x 1 cm) both at the top and the bottom. Top half of the symmetrical physical model is shown in Fig.1. Water, as it flows though the channel, exchanges heat with the upper and lower PCM along its flow path. The upper half can be considered as a rectangular enclosure heated from below, in which case the heat transfer is controlled by convection and conduction. But, there can be only conduction heat transfer in the case of the lower PCM as it being heated from above. In order to study the natural convection effect, in the present work, only the upper half is modeled for numerical analysis. During charging process, hot water flows from the left end to the right end of the inner tube and during the discharge mode the cold water flows from the left end to the right end (same as hot water flow direction). The outer walls of the PCM channel are well insulated. In the present work, paraffin wax and paraffin wax with Alumina (Al_2O_3) and with Copper oxide (CuO) in different compositions varying from 1-5% (by volume) are used as PCMs and water is used as HTF respectively.

Assumptions made in the present study are: (a) top half of the 2-D model with natural convection is analysed, (b) flow of HTF through the channel is laminar, (c) thermal losses through the outer walls of the PCM channel is negligible, (d) heat transfer in the PCM is both conduction and convection controlled, (e) thermophysical properties of the PCM are different for the solid and liquid phases, (f)

* Corresponding author, Email: a_valanarasu@yahoo.com
† Currently associated with Minerals Metals Materials Technology Centre (M3TC), National University of Singapore. Email: ap.sasmito@gmail.com

DOI: 10.5098/hmt.v2.4.3005 ISSN: 2151-8629

thermophysical properties of PCM and HTF are temperature dependent and (g) volume change of PCM is negligible.

The mathematical model comprises two component, viz., water flows and PCM storage, which allows for conjugate heat transfer between carrier fluid (water) and PCM. During charging, the hot water flows through the channel, the heat is then transferred to the PCM to store the energy as latent heat (melt). While at discharging, cool water flows at the channel to take heat from PCM. Initially, the PCM at the molten state and then solidified once the heat is taken away. Note that the three-dimensional physical model is reduced to two-dimensional symmetry model to save computational cost. Since this work relates only to laminar flow, a precise numerical solution is adequate to simulate reality very closely.

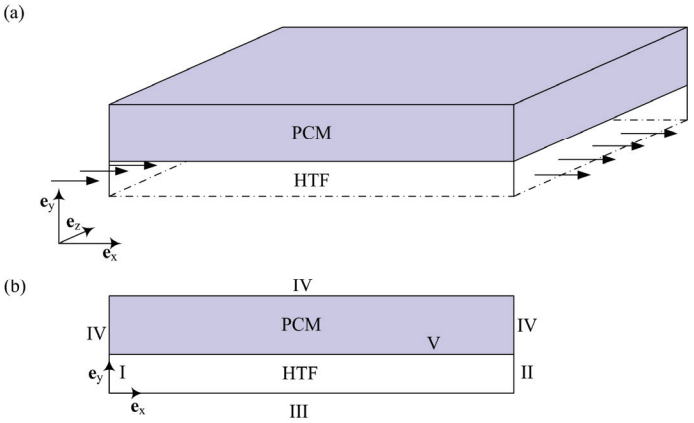

Fig. 1 Schematic of (a) phase change material thermal energy storage; (b) two-dimensional computational domain for conjugate PCM heat transfer. The boundaries are marked with roman numerals: I HTF inlet; II HTF outlet; III symmetry; IV wall/insulation; V interface.

.

2.1. Governing equations

2.1.1. Heat transfer fluid (HTF)

In the HTF, fluid flow and convective heat transfer are taken into consideration. The conservation equations of mass, momentum and energy are given by (Kurnia *et al.* 2011a and Kurnia *et al.* 2011b)

$$\frac{\partial \rho_{\mathrm{w}}}{\partial t} + \nabla \cdot \left(\rho_{\mathrm{w}} \mathbf{u} \right) = 0 \tag{1}$$

$$\frac{\partial}{\partial t}\left(\rho_{\mathrm{w}} \mathbf{u} \right) + \nabla \cdot \left(\rho_{\mathrm{w}} \mathbf{u} \otimes \mathbf{u} \right) = -\nabla p + \nabla \cdot \left(\mu_{\mathrm{w}} \left(\nabla \mathbf{u} + \left(\nabla \mathbf{u} \right)^{\mathbf{T}} \right) \right) \tag{2}$$

$$\frac{\partial}{\partial t}\left(\rho_{\mathrm{w}} c_{\mathrm{p,w}} T \right) + \nabla \cdot \left(\rho_{\mathrm{w}} c_{\mathrm{p,w}} \mathbf{u} T \right) = \nabla \cdot \left(k_{\mathrm{w}} \nabla T \right) \tag{3}$$

where the thermophysical properties of water were obtained as polynomial functions of temperature (Kurnia 2011a and Kurnia 2011b). The water density is defined by

$$\rho_{\mathrm{w}} = -3.570 \times 10^{-3} T^2 + 1.88T + 753.2 \tag{4}$$

while the water viscosity is given by

$$\mu_{\mathrm{w}} = 2.591 \times 10^{-5} \times 10^{\frac{238.3}{T-143.2}} \tag{5}$$

and the thermal conductivity of water is calculated from

$$k_{\mathrm{w}} = -8.354 \times 10^{-6} T^2 + 6.53 \times 10^{-3} T - 0.5981 \tag{6}$$

The specific heat of water is considered constant at

$$c_{\mathrm{p,w}} = 4200 \tag{7}$$

For sake of brevity, we refer the reader to Nomenclature for symbols and notations

2.1.2. PCM storage

In the storage, fluid flow, heat transfer and phase change processes of PCM with nanoparticle are taken into consideration. The conservation of mass, momentum and energy are given by

$$\frac{\partial}{\partial t}\left(\rho_{\text{n-pcm}} \right) + \nabla \cdot \left(\rho_{\text{n-pcm}} \mathbf{u} \right) = 0 \tag{8}$$

$$\frac{\partial}{\partial t}\left(\rho_{\text{n-pcm}} \right) + \nabla \cdot \left(\rho_{\text{n-pcm}} \mathbf{u} \otimes \mathbf{u} \right) = \nabla \cdot \sigma + \rho_{\text{n-pcm}} \mathbf{g} + \mathbf{S}_{\mathrm{mom}} \tag{9}$$

where

$$\boldsymbol{\sigma} = -p\mathbf{I} + \nabla \cdot \left(\mu_{\text{n-pcm}} \left(\nabla \mathbf{u} + \left(\nabla \mathbf{u} \right)^{\mathbf{T}} \right) \right) \tag{10}$$

$$\frac{\partial}{\partial t}\left(\rho_{\text{n-pcm}} H_{\text{n-pcm}} \right) + \nabla \cdot \left(\rho_{\text{n-pcm}} \mathbf{u} H_{\text{n-pcm}} \right) = \nabla \cdot \left(k_{\text{n-pcm}} \nabla T \right) \tag{11}$$

In the above equations, we implement enthalpy-porosity formulation which is represented by additional source terms in momentum equation, $\mathbf{S}_{\mathrm{mom}}$ and accounted for latent heat of PCM in the enthalpy term of energy equation, $H_{\text{n-pcm}}$, defined as

$$H_{\text{n-pcm}} = h_{\text{n-pcm}} + \Delta H_{\text{n-pcm}} \tag{12}$$

where $h_{\text{n-pcm}}$ is the sensible heat, given by

$$h_{\text{n-pcm}} = h_{\text{n-cpm}}^{\mathrm{ref}} + \int_{T^{\mathrm{ref}}}^{T} c_{\text{p,n-pcm}} dT \tag{13}$$

The latent heat of nano-PCM suspension is estimated by

$$\Delta H_{\text{n-pcm}} = \left(1 - \omega_{\mathrm{np}} \right) \beta L \tag{14}$$

Where L is the latent heat of PCM, ω_{np} is the mass fraction of nanoparticle, and β is the melted mass fraction of PCM, given by

$$\begin{aligned} \beta &= 0 && \text{if } T < T_{\text{solidius}} \\ \beta &= 1 && \text{if } T > T_{\text{liquidius}} \\ \beta &= \frac{T - T_{\text{solidius}}}{T_{\text{liquidius}} - T_{\text{solidius}}} && \text{if } T_{\text{solidius}} < T < T_{\text{liquidius}} \end{aligned} \tag{15}$$

Furthermore, the enthalpy-porosity formulation treats the mushy region (partially solidified) as a porous medium. The porosity in each cell is set to equal to the liquid fraction in the cell. In fully solidified region, the porosity is equal to zero, which extinguishes the velocities in this region. The source term due to the reduced porosity in the mushy zone is approximated by

$$\mathbf{S}_{\mathrm{mom}} = \frac{\left(1 - \beta \right)^2}{\left(\beta^3 + 0.001 \right)} H \mathbf{u} \tag{16}$$

where H is mushy zone constant.

2.2. Constitutive relations

Thermophysical properties of the nano-PCM are functions of concentration of nanoparticles, PCM and temperature, similar to our previous work (Sasmito *et al.* 2011). The PCM considered in this study is paraffin wax; the density, ρ_{pcm}, is given by (Kandasamy *et al.* 2008)

$$\rho_{\mathrm{pcm}} = \frac{750}{0.001\left(T - 319.15 \right) + 1} \tag{17}$$

DOI: 10.5098/hmt.v2.4.3005 ISSN: 2151-8629

The nano-PCM suspension density is defined as (Sasmito *et al.* 2011)

$$\rho_{\text{n-pcm}} = \phi_{\text{np}}\rho_{\text{np}} + \left(1-\phi_{\text{np}}\right)\rho_{\text{pcm}} \tag{18}$$

where ϕ_{np} and ρ_{np} is the volumetric fraction and density of nanoparticle, respectively. The specific heat of nano-PCM is assumed to be a weighted average of the PCM and nanoparticle,

$$c_{\text{p,n-pcm}} = \frac{\phi_{\text{np}}\rho_{\text{np}}c_{\text{p,np}} + \left(1-\phi_{\text{np}}\right)\rho_{\text{pcm}}c_{\text{p,pcm}}}{\rho_{\text{n-pcm}}} \tag{19}$$

The PCM thermal conductivity is estimated by

$$\begin{aligned} k_{\text{pcm}} &= k_{\text{pcm}}^{(\text{s})} \qquad \text{if } T < T_{\text{solidius}} \\ k_{\text{pcm}} &= k_{\text{pcm}}^{(\text{l})} \qquad \text{if } T > T_{\text{liqidius}} \end{aligned} \tag{20}$$

The effective thermal conductivity of the nanoPCM, which includes the effects of particle size, particle volume fraction and temperature dependence as well as properties of the base PCM and the particle subject to Brownian motion, given by (Vajjha *et al.* 2010)

$$\begin{aligned} k_{\text{n-pcm}} = {} & \frac{k_{\text{np}} + 2k_{\text{pcm}} - 2\left(k_{\text{pcm}} - k_{\text{np}}\right)\phi_{\text{np}}}{k_{\text{np}} + 2k_{\text{pcm}} + \left(k_{\text{pcm}} - k_{\text{np}}\right)\phi_{\text{np}}}k_{\text{pcm}} \\ & + \beta k_1 \varsigma \phi_{\text{np}}\rho_{\text{pcm}}c_{\text{p,pcm}}\sqrt{\frac{\kappa T}{\rho_{\text{np}}d_{\text{np}}}}f\left(T,\phi_{\text{np}}\right) \end{aligned} \tag{21}$$

Where d_{np} is the nanoparticle diameter, k_1 is the Brownian motion constant, κ is the Boltzmann constant. The first part of Eq. (21) is derived from the Maxwell model while the second part accounts for Brownian motion, which causes the temperature dependence of the effective thermal conductivity. Note that there is a correction factor, β, in the Brownian motion term, since there should be no Brownian motion in the solid phase. Its value is defined to be the same as for liquid fraction, β, in equation (15). The empirical relation is used to account for Brownian motion, given by (Vajjha *et al.* 2010)

$$\varsigma = \varsigma_1\left(100\phi_{\text{np}}\right)^{\varsigma_2} \tag{22}$$

$$f\left(T,\phi_{\text{np}}\right) = \left(c_1\phi_{\text{np}} + c_2\right)T \,/\, T_{\text{ref}} + \left(c_3\phi_{\text{np}} + c_4\right) \tag{23}$$

The PCM viscosity is defined as

$$\mu_{\text{pcm}} = 0.001\exp\left(-4.25 + 1790 \,/\, T\right) \tag{24}$$

and the viscosity of nano-PCM is approximated by

$$\mu_{\text{n-pcm}} = C_1\exp\left(C_2\phi_{\text{np}}\right)\mu_{\text{pcm}} \tag{25}$$

The nano-PCM mass fraction is given by

$$\omega_{\text{np}} = \frac{\phi_{\text{np}}\rho_{\text{n-pcm}}}{\left(\rho_{\text{pcm}} + \phi_{\text{np}}\left(\rho_{\text{n-pcm}} - \rho_{\text{pcm}}\right)\right)} \tag{26}$$

2.3. Initial and boundary conditions

The boundary conditions are prescribed as follows:

- *Inlet* (I): At the inlet, we specify inlet velocity and inlet temperature

$$\begin{aligned} u = U^{\text{in}},\ T = T^{\max} \quad & \text{for charging} \\ u = U^{\text{in}},\ T = T^{\min} \quad & \text{for discharging} \end{aligned} \tag{27}$$

- *Outlet* (II): At the outlet, we set pressure and streamwise gradient of temperature to zero; the outlet velocity is not known a priori but needs to be iterated from the neighboring computational cells.

$$p = p^{\text{out}},\ \mathbf{n}\cdot\left(k_{\text{w}}\nabla T\right) = 0 \tag{28}$$

- *Symmetry* (III): At the symmetry, we specify zero shear stress, no normal flow and no heat flux condition.

$$\begin{aligned} &\left(\mathbf{n}\cdot\nabla\right)\left(\mathbf{u}\cdot\mathbf{t}\right) = 0, \\ &\mathbf{n}\cdot\mathbf{u} = 0, \\ &\mathbf{n}\cdot\nabla T = 0 \end{aligned} \tag{29}$$

- *Walls* (IV): At walls, we set no slip and no heat flux condition.

$$\mathbf{u} = \mathbf{0},\ \mathbf{n}\cdot\nabla T = 0 \tag{30}$$

- *Interface* (V): At the interface, we specify no-slip condition for velocities and coupled temperature to allow for conjugate heat transfer.

$$\mathbf{u} = \mathbf{0},\ T_V^{+} = T_V^{-} \tag{31}$$

The initial conditions are defined as follows:

- *Charging*: During charging, we set initial temperature to be the same as ambient temperature.

$$\text{at } t = 0,\ T = T^{\min},\ \mathbf{u} = \mathbf{0} \tag{32}$$

- *Discharging*: During discharging, the initial temperature is set to be equal to maximum temperature of hot water.

$$\text{at } t = 0,\ T = T^{\max},\ \mathbf{u} = \mathbf{0} \tag{33}$$

In this paper, a constant velocity of water at Re 1000 is prescribed at the inlet for comparison purposes.

Table 1. Base-case and operating parameters (Sasmito *et al.* 2011)

Parameter	*Value*	*Unit*
$c_{\text{p,np,Al}_2\text{O}_3}$, $c_{\text{p,np,CuO}}$	765, 540	J kg^{-1} K
$c_{\text{p,pcm}}$	2890	J kg^{-1} K
$d_{\text{np,Al}_2\text{O}_3}$, $d_{\text{np,CuO}}$	(59, 29) × 10^{-9}	m
$k_{\text{np,Al}_2\text{O}_3}$, $k_{\text{np,CuO}}$	36, 18	W m^{-1} K^{-1}
$k_{\text{pcm}}^{(\text{s})}$, $k_{\text{pcm}}^{(\text{l})}$	0.21, 0.12	W m^{-1} K^{-1}
k_1	5 × 10^{4}	-
κ	1.381 × 10^{-23}	J K^{-1}
L	173400	J kg^{-1}
H	1 × 10^{5}	-
$\rho_{\text{np,Al}_2\text{O}_3}$, $\rho_{\text{np,CuO}}$	3600, 6510	kg m-3
p_{out}	101325	Pa
T_{ref}	298.15	K
$T^{\min}$, $T^{\max}$	300, 350	K
T_{solidius}, $T_{\text{liquidius}}$	319.15, 321.15	K
c_1, c_2	(28.217, 3.917) × 10^{-3}	-
c_3, c_4	(-30.669, -3.91123) × 10^{-3}	-
C_1 (Al_2O_3, CuO)	0.9830, 0.9197	-
C_2 (Al_2O_3, CuO)	12.959, 22.8539	-
ς_1 (Al_2O_3, CuO)	8.4407, 9.881	-
ς_2 (Al_2O_3, CuO)	-1.07304, -0.9446	-

3. COMPUTATIONAL METHODOLOGY

The model for the numerical study (Fig. 1 (b)) was created using pre-processor software GAMBIT 2.3.16. Meshing of the numerical domain was generated and the boundary conditions applied at appropriate surfaces. The computational domain was resolved with a fine structured mesh near the wall to resolve the boundary layer and an increasingly coarser mesh in the rest of the domain in order to reduce the computational time. After grid independence test, 14000 and 15000 grid cells are selected, respectively, for the PCM zone and the HTF zone. The GAMBIT model is then exported to FLUENT for numerical solution.

The *pressure-based* method within version 6.3.26 of the commercial code FLUENT was utilized for solving the governing equations. User-defined functions (UDF) were written in C language to account for temperature-dependence of the thermo-physical properties of paraffin wax, nanoparticle and water. The time step for integrating the temporal derivatives was set to 0.01 s. The *first-order upwind* differencing scheme was used for solving the momentum and energy equations, whereas the PRESTO scheme was adopted for the pressure correction equation. The under-relaxation factors for the velocity components, pressure correction and thermal energy were 0.5, 0.3 and1 respectively. Convergence criteria were set at 10^{-3} for continuity and momentum, and 10^{-6} for thermal energy.

An enthalpy-porosity technique is used in FLUENT for modelling the solidification/melting process. In this technique, the liquid melt fraction in each cell is computed every iteration, based on enthalpy balance. The mushy zone is the region where the porosity increases from 0 to 1 as the PCM melts. When the region is complete solid, the porosity is zero and also the flow velocity in that zone also drops to zero

4. RESULTS AND DISCUSSION

The numerical simulations were carried out for typical conditions found in PCM thermal energy storage. The base-case conditions together with the physical parameters are listed in Table 1. In the following, we will examine the effect of nanoparticle suspended in the PCM with respect to the thermophysical properties and heat transfer rate at various volumetric nanoparticle concentrations during charging and discharging. Advantages and limitation is also discussed in the light of numerical results.

4.1. Thermo-physical properties

The computed dynamic viscosity and effective thermal conductivity of paraffin wax dispersed with 0%, 1%, 3%, 5% and 10 % by volume of nanoparticles both Al_2O_3 and CuO (nanoPCM) using the above equations (Eqs. 21 and 25) are plotted as a function of temperature and volumetric concentration in Fig.2 and Fig.3.

It is seen from Fig. 2(a) and 3(a) that the thermal conductivity of nanoPCM is greater than the simple PCM. Hence, nanoPCM has higher heat transfer rate compared to the same mass of simple PCM. But, as shown in Fig. 2(b) and 3(b), viscosity of nanoPCM increases with the increase in the volumetric concentration of nanoparticles. The increase in dynamic viscosity is greater for CuO nanoparticles compared with Al_2O_3 nanoparticles in paraffin wax. The enhancement in the dynamic viscosity for the nanoPCM may play a key role in the natural convection dominated melting of nanoPCM.

The variation in thermal conductivity and dynamic viscosity of nanoPCM with temperature and volume fraction of Al_2O_3 agree well with the experimental results reported in Ref. (Ho and Gao, 2009).

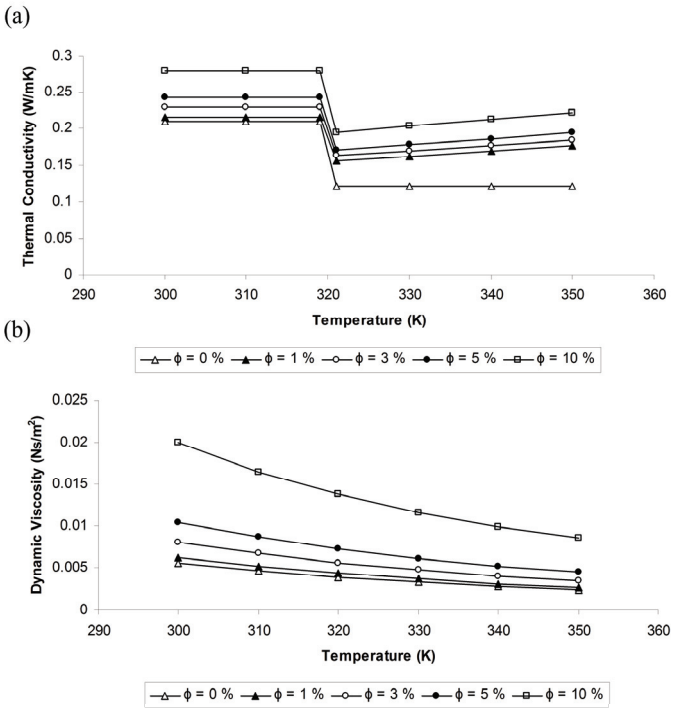

Fig. 2 Thermo-physical properties of nanoPCM comprising paraffin wax and Al_2O_3 for (a) thermal conductivity and (b) dynamic viscosity for volumetric concentration of nanoparticle 0% [Δ], 1% [▲], 3% [○], 5% [●], and 10% [□].

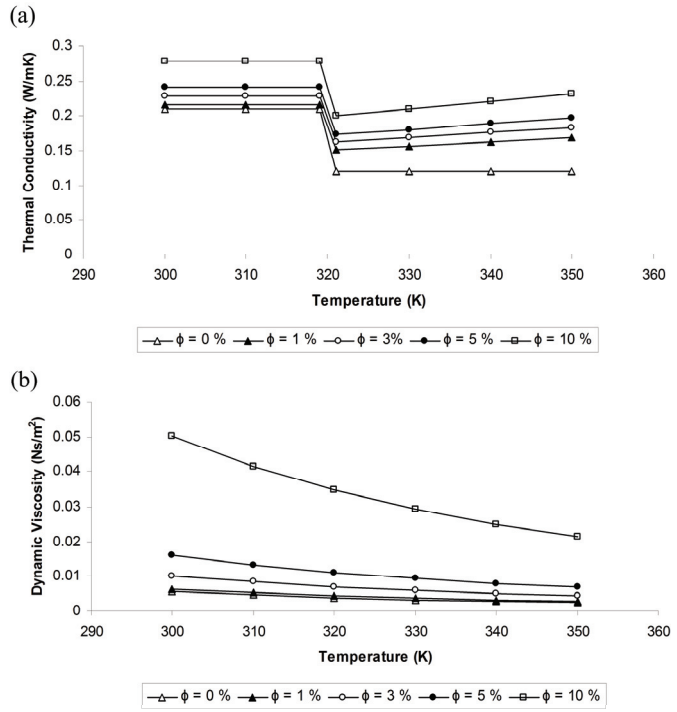

Fig. 3 Thermo-physical properties of nanoPCM comprising paraffin wax and CuO for (a) thermal conductivity and (b) dynamic viscosity for volumetric concentration of nanoparticle 0% [Δ], 1% [▲], 3% [○], 5% [●], and 10% [□].

4.2. Heat transfer performance

The melting and solidification rate of nanoparticle enhanced paraffin wax is examined for various volumetric concentrations viz. 0%, 1%, 3% and 5% of Al_2O_3 and CuO nanoparticles. The time evolution of melting of paraffin wax without and with nanoparticles is shown in Fig. 4 and Fig. 5.

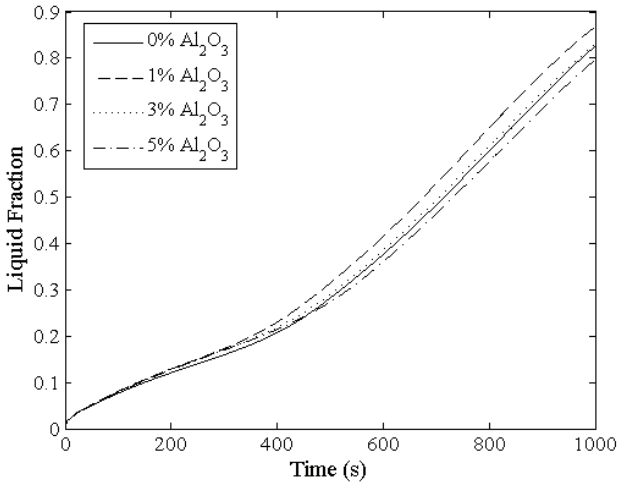

Fig. 4 Melting processes of nanoPCM (paraffin wax and Al_2O_3) at nanoparticle concentration of 0% [—], 1% [---], 3% [···], and 5% [– · –].

It is expected that additional nanoparticle into paraffin wax enhances the heat transfer performance; this is indeed the case for low nanoparticle concentration of 1%, as can be inferred from Figs. 4 and 5. It is noted that the nanoPCM melts faster only marginally by 4.8% and 2.9% for 1% Al2O3 and CuO, respectively, compared to that for pure paraffin wax (Figs. 4 and 5). This exemplifies the enhancement, albeit small, in the thermal conductivity of paraffin wax with Al_2O_3 nanoparticle.

As the nanoparticle concentration increased, an adverse effect is seen: the time required for melting at higher nanoparticle concentration is longer than that for pure and low concentration (1%) of nano- PCM. This is attributed to the fact that nanoPCM viscosity increases significantly as nanoparticle concentration increased (Ho and Gao, 2009). The increase of dynamic viscosity for CuO nanoPCM is twice that for Al_2O_3 nanoPCM (see Figs. 2b and 3b). As the natural convection dominates the heat transfer rate in the melting process, higher the viscosity reduces the buoyancy more which, in turn, slower the melting process. We note that the melting rate for Al_2O_3 is somewhat slower by around 1% and 3% for nanoparticle concentration of 3 and 5%, respectively. While the longer melting time is seen for CuO nanoparticle; notably that the melting time increases up to ~ 5% and 10% for CuO nanoparticle concentration of 3 and 5%, respectively. Closer inspection reveals that there is no significant difference on heat transfer rate at first 400 s since the heat transfer is controlled by conduction mode. Once more PCM melted, the dominant mechanism shifts to natural convection where the viscosity effect is greater. This is further mirrored by lower heat transfer rate for higher nanoparticle concentration due to viscosity increase at time higher than 400s (Fig. 5).

A further point of interest in this study is the solidification process/discharging. In essence, conduction heat transfer controls the heat transfer rate during solidification. As thermal conductivity of PCM is considerably low (~ 0.12 to 0.21 W m^{-1} K^{-1}), the time required for solidification is expected to be longer than that of melting process. Indeed, the computed results indicate that the overall time required for complete solidification is doubled than that for melting process (see Figs. 4 and 6). The conduction heat transfer dominates the solidification process; whence adding nanoparticle enhances thermal conductivity, whilst increasing dynamic viscosity of suspension.

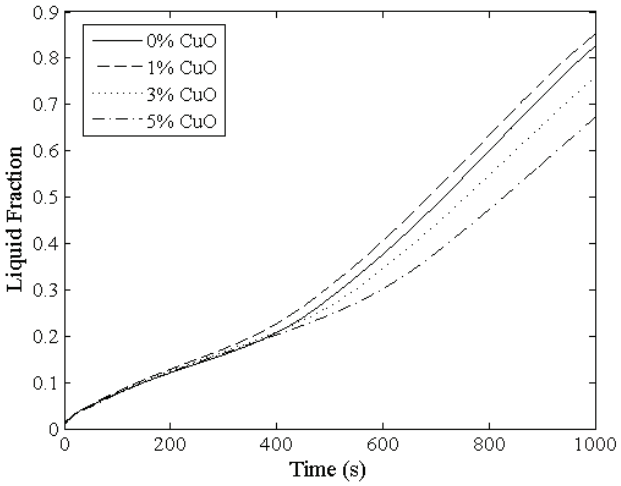

Fig. 5 Melting processes of nanoPCM (paraffin wax and CuO) at nanoparticle concentration of 0% [—], 1% [---], 3% [···], and 5% [– · –].

Khodadadi and Hosseinizadeh (2007), albeit use water as PCM fluid and Copper nanoparticle in their simulation, found that the solidification time speeded-up by ~ 33% and 50% as they add 10% and 20% nanoparticle, respectively. In contrast, our computed results show that solidification rate for PCM only increases marginally with increase in volumetric composition of Al_2O_3; and even decreases with increase in volumetric concentration of CuO nanoparticles in paraffin wax.

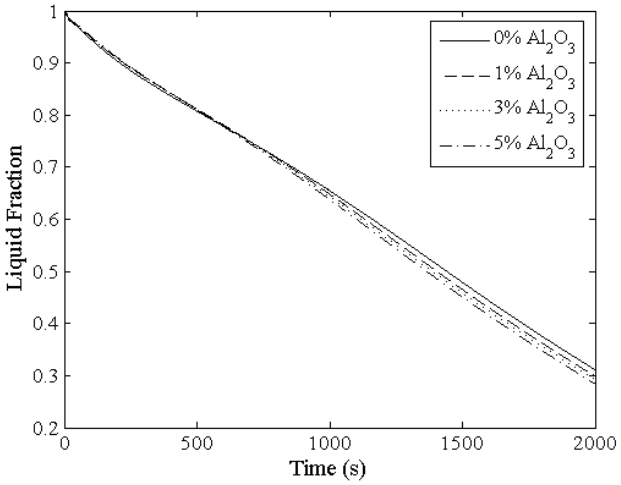

Fig. 6 Solidification processes of nanoPCM (paraffin wax and Al_2O_3) at nanoparticle concentration of 0% [—], 1% [---], 3% [···], and 5% [– · –].

It is observed that the solidification time only slightly expedites by up to 4% for additional 5% Al_2O_3 nanoparticle, as can be seen in Fig. 6, and slower by ~ 7% for additional 5% CuO nanoparticle (see Fig, 7). This can be attributed to the fact that present simulation considers all the thermophysical properties to be function of temperature and nanoparticle concentration; whereas Khodadadi and Hosseinizadeh (2007) used constant thermophysical. Also, they considered water as their PCM where thermal conductivity is assumed to be the same for both solid and liquid phase, while present simulation consider thermal conductivity as function of phase (liquid/solid), temperature and nanoparticle concentration. The constant thermophysical properties together with single thermal conductivity

DOI: 10.5098/hmt.v2.4.3005 ISSN: 2151-8629

assumption of water by Khodadadi and Hosseinizadeh (2007) may lead to over-predict the heat transfer performance of nanoPCM.

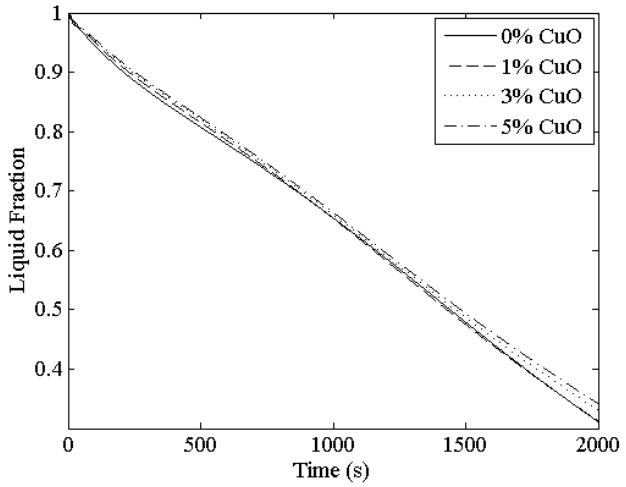

Fig. 7 Solidification processes of nanoPCM (paraffin wax and CuO) at nanoparticle concentration of 0% [—], 1% [---], 3% [···], and 5% [– · –].

From the foregoing analysis, it is found that 1% volumetric concentration of nanoparticle enhances the performance of paraffin wax compared to higher concentrations. It is also noted that enhancement is greater for Al_2O_3 compared with CuO (see Table 2). It is due to the reasons that the increase in the dynamic viscosity of Al_2O_3 nanoparticle is lower (Fig. 2b) than CuO nanoparticle (Fig. 3b), which plays a key role in melting process. Moreover, the thermal conductivity of Al_2O_3 is greater (Table 1), which is important for the conduction dominated solidification process, compared to that of CuO.

Intuitively, adding larger amount of nanoparticle in the PCM enhances thermal conductivity; however, care has to be taken as it also increases the friction factor (viscosity), reduces the available latent heat of PCM and may reduce the stability of nanoPCM due to agglomeration and sedimentation. Thus, selecting a proper nanoparticle material and its concentration is essential to improve heat transfer performance of PCM in terms of both melting and solidification processes.

Table 2. Summary of heat transfer performance

ϕ_{np} *[%]*	*t fully melt at charging [s]*	*t fully soidified at discharging [s]*	$\Delta H_{n\text{-}pcm,max}$ *[J kg^{-1}]*
0%	1313	2771	173400
1% Al_2O_3	1293	2731	171614
3% Al_2O_3	1316	2709	167614
5% Al_2O_3	1361	2674	163150
1% CuO	1328	2801	171533
2% CuO	1425	2906	167036
3% CuO	1575	2976	161606

5. CONCLUSION

In the present work, a numerical investigation is carried out to estimate the effect on thermal performance of paraffin wax due to the enhancement in thermal conductivity using alumina(Al_2O_3) and copper oxide (CuO) nanoparticles.

The effect of volumetric concentration of the nanoparticles on the melting and solidification performance is examined and compared between the two nanoparticles. From the present study it has been confirmed that the thermal performance of paraffin wax is enhanced only marginally with the dispersion of Al_2O_3 and CuO nanoparticles. The overall performance i.e. both melting and solidification processes of paraffin wax is better for lower concentration of nanoparticles. The benefit is greater for Al_2O_3 compared to CuO due to the reasons that the increase in the dynamic viscosity with Al_2O_3 is lower, which plays a key role in melting process and the thermal conductivity of Al_2O_3 is greater, which is important for the conduction dominated solidification process, compared with that of CuO. Overall, however, the use of nanoparticles can enhance energy charge and discharge rates only nominally. It is unlikely that this will be economically justifiable for low cost storage especially as the stability of nanoPCMs subjected to a large number of melting/freezing cycles has not been investigated yet.

ACKNOWLEDGEMENT

Dr. A. Valan Arasu gratefully acknowledges the financial support of the Department of Science and Technology, New Delhi, INDIA in the form of BOYSCAST Fellowship.

NOMENCLATURE

c_p	specific heat [J kg^{-1} K^{-1}]
C	viscosity parameter constants
d	diameter [m]
g	gravity [m s^{-2}]
h	Sensible heat [Jkg^{-1}]
H	total enthalpy [J kg^{-1}]
ΔH	enthalpy of phase change [J kg^{-1}]
k	Brownian motion constant
k	thermal conductivity [W m^{-1} K^{-1}]
κ	Boltzmann constant [J K^{-1}]
H	mushy zone constant
L	length [m]
L	latent heat [J kg^{-1}]
p	pressure [Pa]
Re	Reynolds number
S	source/sink term
T	temperature [K]
t	time [s]
U, **u**, u, v	velocity [m s^{-1}]

Greek

β	melted fraction
ς	Brownian motion parameter
ρ	density [kg m^{-3}]
ϕ	volume fraction
σ	total stress tensor
μ	dynamic viscosity [Pa s]
ω	mass fraction

Subscript

liquidius	liquidius
pcm	phase change material
ref	reference
mom	momentum
n-pcm	nano-phase change material
np	nanoparticle
solidius	solidius
w	water

Superscript

in	inlet
l	liquid
ref	reference
out	outlet
min	minimum
max	maximum
s	solid

Global Digital Central
ISSN: 2151-8629

REFERENCES

Cabeza, L.F., Mehling, H., Hiebler,S., and Ziegler, F., 2002, "Heat transfer enhancement in water when used as PCM in thermal energy storage," *Applied Thermal Engineering*, 22, 1141–1151. http://dx.doi.org / doi:10.1016/S1359-4311(02)00035-2

Calmidi, V.V., and Mahajan, R.L., 1999, "The effective thermal conductivity of high porosity fibrous metal foam," *Journal of Heat Transfer*, 121, 466–471. http://dx.doi.org / doi:10.1115/1.2826001

Chow, L.C., Zhong, J.K., 1996, "Thermal conductivity enhancement for Phase change storage media," *International Communications in Heat and Mass Transfer*, 23, 91-100. http://dx.doi.org / doi:10.1016/0735-1933(95)00087-9

Fukai, J., Hamada, Y., Morozumi, Y., and Miyatake, O., 2002, "Effect of carbon-fiber brushes on conductive heat transfer in phase change materials," *International Journal of Heat Mass Transfer*, 45, 4781–4792. http://dx.doi.org / doi:10.1016/S0017-9310(02)00179-5

Fukai, J., Kanou, M., Kodama, Y., and Miyatake, O., 2000, "Thermal conductivity enhancement of energy storage media using carbon fibers," *Energy Conversion Management*, 41, 1543–1556. http://dx.doi.org / doi:10.1016/S0196-8904(99)00166-1

Ho, C.J., and Gao, T.Y., 2009, "Preparation and thermophysical properties of nanoparticle-in-paraffin emulsion as phase change material," *International Communications in Heat and Mass Transfer*, 36, 467-470. http://dx.doi.org / doi:10.1016/j.icheatmasstransfer.2009.01.015

Hoogendoorn, C.J., and Bart, G.C.J.,1992, "Performance and modelling of latent heat stores,", *Solar Energy*, 48, 53–58. http://dx.doi.org / doi:10.1016/0038-092X(92)90176-B

http://www.fluent.com.

Kenisarin, M., and Mahkamov, K., 2007, "Solar energy storage using phase change materials," *Renewable and Sustainable Energy Reviews*, 11, 1913–65. http://dx.doi.org / doi:10.1016/j.rser.2006.05.005

Kim, S., and Drzal, L.T., 2009, "High latent heat storage and high thermal conductive phase change materials using exfoliated graphite nanoplatelets," *Solar Energy Materials and Solar Cells*, 93, 136–142. http://dx.doi.org / doi:10.1016/j.solmat.2008.09.010

Khodadadi, J.M., and Hosseinizadeh, S.F., 2007, "Nanoparticle-enhanced phase change materials (NEPCM) with great potential for improved thermal energy storage," *International Communication in Heat Mass Transfer*, 34, 534–543. http://dx.doi.org / doi:10.1016/j.icheatmasstransfer.2007.02.005

Kurnia, J.C., Sasmito, A.P., Mujumdar, A.S., 2011a, "Numerical investigation of laminar heat transfer performance of various cooling channel designs," *Aplied Thermal Engineering*, 31, 1293–1304. http://dx.doi.org / doi:10.1016/j.applthermaleng.2010.12.036

Kurnia, J.C., Sasmito, A.P., Mujumdar, A.S., 2011b, "Evaluation of heat transfer performance of helical coils of non-circular tubes," *Journal of Zhejiang University Science A*, 12, 63–70. http://dx.doi.org / doi: 10.1631/jzus.A1000296

Mettawee, E.S., and Assassa, G.M.R., 2007, "Thermal conductivity enhancement in a latent heat storage system," *Solar Energy*, 81, 839–845. http://dx.doi.org / doi:10.1016/j.solener.2006.11.009

Pincemin, S., Py, X., Olives, R., Christ, M., and Oettinger, O., 2008, "Elaboration of conductive thermal storage composites made of phase change materials and graphite for solar power plant," *ASME Journal of Solar Energy Engineering*, 130, 11005–11009. http://dx.doi.org / doi:10.1115/1.2804620

Ravi Kandasamy, Wang, X.Q., and Mujumdar, A.S., 2008, "Transient cooling of electronics using phase change material (PCM)-based heat sinks," *Applied Thermal Engineering*, 28, 1047–1057. http://dx.doi.org / doi:10.1016/j.applthermaleng.2007.06.010

Sasmito, A.P., Kurnia, J.C., and Mujumdar, A.S., 2011, "Numerical Evaluation of Laminar Heat Transfer Enhancement in Nanofluid Flow in Coiled Square Tubes," *Nanoscale Research Letters*, in press.

Sharma, S.D., and Sagara, K., 2005, "Latent heat storage materials and systems: a review." *International Journal of Green Energy*,2,1–56. http://dx.doi.org / doi:10.1081/GE-200051299

Tayeb, A.M., 1996, "Use of some industrial wastes as energy storage media," *Energy Conversion Management*, 37, 127–133. http://dx.doi.org / doi:10.1016/0196-8904(95)00171-9

Vajjha, R.S., Das, D. K., Namburu, P. K., 2010, "Numerical study of fluid dynamic and heat transfer performance of Al_2O_3 and CuO nanofluids in the flat tubes of a radiator," *International Journal of Heat Fluid Flow*, 31, 613-621. http://dx.doi.org / doi:10.1016/j.ijheatfluidflow.2010.02.016

Velraj, R., Seeniraj, R.V., Hafner, B., Faber, C., and Schwarzer, K., 1999, "Heat transfer enhancement in latent heat storage system," *Solar Energy*, 65, 171–180. http://dx.doi.org / doi:10.1016/S0038-092X(98)00128-5

Weaver, J.A., and Viskanta, R., 1986, "Melting of frozen, porous media contained in a horizontal or a vertical, cylindrical capsule,", *International Journal of Heat Mass Transfer,* 29, 1943–1951. http://dx.doi.org / doi:10.1016/0017-9310(86)90013-X

Zalba, B., Marin, J.M., Cabeza, L.F., and Mehling, H., 2003, "Review on thermal energy storage with phase change: materials, heat transfer analysis and applications," *Applied Thermal Engineering*, 23, 251–83. http://dx.doi.org / doi:10.1016/S1359-4311(02)00192-8

Zeng, J.L., Sun, L.X., Xu, F., Tan, Z.C., Zhang, Z.H., and Zhang, J., 2007, "Study of a PCM based energy storage system containing Ag nanoparticles," *Journal of Thermal Analysis Calorimetry*, 87, 369–373. http://dx.doi.org / doi:10.1007/s10973-006-7783-z